

Probing non-standard decoherence effects with solar and KamLAND neutrinos

G.L. Fogli¹, E. Lisi¹, A. Marrone¹, D. Montanino², and A. Palazzo^{3,1}

¹ *Dipartimento di Fisica and Sezione INFN di Bari,
Via Amendola 173, 70126, Bari, Italy*

² *Dipartimento di Fisica and Sezione INFN di Lecce
Via Arnesano, 73100 Lecce, Italy*

³ *Astrophysics, Denys Wilkinson Building,
Keble Road, OX1 3RH,
Oxford, United Kingdom*

Abstract

It has been speculated that quantum gravity might induce a “foamy” space-time structure at small scales, randomly perturbing the propagation phases of free-streaming particles (such as kaons, neutrons, or neutrinos). Particle interferometry might then reveal non-standard decoherence effects, in addition to standard ones (due to, e.g., finite source size and detector resolution.) In this work we discuss the phenomenology of such non-standard effects in the propagation of electron neutrinos in the Sun and in the long-baseline reactor experiment KamLAND, which jointly provide us with the best available probes of decoherence at neutrino energies $E \sim \text{few MeV}$. In the solar neutrino case, by means of a perturbative approach, decoherence is shown to modify the standard (adiabatic) propagation in matter through a calculable damping factor. By assuming a power-law dependence of decoherence effects in the energy domain (E^n with $n = 0, \pm 1, \pm 2$), theoretical predictions for two-family neutrino mixing are compared with the data and discussed. We find that neither solar nor KamLAND data show evidence in favor of non-standard decoherence effects, whose characteristic parameter γ_0 can thus be significantly constrained. In the “Lorentz-invariant” case $n = -1$, we obtain the upper limit $\gamma_0 < 0.78 \times 10^{-26} \text{ GeV}$ at 95% C.L. In the specific case $n = -2$, the constraints can also be interpreted as bounds on possible matter density fluctuations in the Sun, which we improve by a factor of ~ 2 with respect to previous analyses.

PACS numbers: 14.60.Pq, 26.65.+t, 03.65.Yz, 04.60.-m

I. INTRODUCTION

Although a satisfactory theory of quantum gravity is still elusive, it has been speculated that it should eventually entail violations of basic quantum mechanics, including the spontaneous evolution of pure states into mixed (decoherent) states [1] through unavoidable interactions with a pervasive and “foamy” space-time fabric at the Planck scale [2]. The pioneering paper [3] showed that such hypothetical source of decoherence might become manifest in oscillating systems which propagate over macroscopical distances, through additional smearing effects in the observable interferometric pattern (besides the usual smearing effects due, e.g., to the finite source size and the detector resolution). However, lacking an “ab initio” theory of quantum gravity decoherence, its effects can only be parameterized in a model-dependent (and somewhat arbitrary) way. Searches with neutral kaon oscillations [3, 4, 5, 6], neutron interferometry [3, 7] and, more recently, neutrino oscillations [8, 9, 10, 11, 12, 13, 14], have found no evidence for such effects so far, and have placed bounds on model parameters.

Quantum gravity effects in neutrino systems have been investigated with increasing attention in the last decade, as a result of the evidence for neutrino flavor oscillations. Early attempts tried to interpret the solar neutrino puzzle [8, 9, 10] or the atmospheric ν anomaly [10] in terms of decoherence. After the first convincing evidence for atmospheric neutrino oscillations [15], a quantitative analysis was performed in [11], considering possible decoherence effects in the $\nu_\mu \rightarrow \nu_\mu$ channel (see also [12]). The phenomenology of terrestrial neutrino experiments has also been investigated in [13, 14]. More recently, prospective studies have focused on decoherence effects in high energy neutrinos [16, 17, 18, 19, 20], observable in next generation neutrino telescopes. Furthermore, more formal aspects of quantum gravity decoherence in neutrino systems have been developed [21, 22, 23, 24, 25, 26, 27]. This is only a fraction of the related literature, which testifies the wide and increasing interest in the subject.

Despite this interest, to our knowledge such decoherence effects have not been systematically investigated in the light of the solar neutrino experiments performed in the last few years. Solar neutrino oscillations [28] dominated by matter effects [29, 30] are currently well established by solar neutrino experiments [31, 32, 33, 34, 35, 36, 37, 38, 39, 40, 41] and have been independently confirmed by the long-baseline reactor experiment KamLAND [42, 43]. The striking agreement between solar and KamLAND results determines a unique solution in the mass-mixing parameter space [the so-called Large Mixing Angle (LMA) solution, see e.g. [44, 45]], provides indirect evidence for matter effects with standard amplitude [46], and generally (although not always [47]) implies that additional, non-standard physics effects may play only a subleading role, if any. In particular, the KamLAND collaboration has exploited the observation of half oscillation cycle in the energy spectrum [43] to exclude decoherence as a dominant explanation of their data.

The main purpose of this paper is then to study decoherence as a *subdominant* effect in solar and KamLAND neutrino oscillations. Modifications of the standard oscillation formulae in the presence of decoherence, and qualitative bounds on decoherence parameters, are discussed in Sec. II and III for KamLAND and solar neutrinos, respectively. Quantitative bounds on subdominant decoherence effects from a joint analysis of solar and KamLAND data are studied in Sec. IV. Implications for decoherence induced by matter fluctuations in the Sun are discussed in Sec. V. The main results are finally summarized in Sec. VI. The solar neutrino flavor evolution in the presence of standard matter effects plus non-standard decoherence is discussed in a technical Appendix.

II. OSCILLATIONS WITH(OUT) DECOHERENCE IN KAMLAND

Here and in the following, we assume the standard notation [48] for neutrino mixing, and set the small mixing angle θ_{13} to zero for the sake of simplicity. For $\theta_{13} = 0$, oscillations in the $\nu_e \rightarrow \nu_e$ channel probed by long-baseline reactor (KamLAND) and by solar neutrinos are driven by only two parameters: the mixing angle θ_{12} and the neutrino squared mass difference $\delta m^2 = m_2^2 - m_1^2$. In particular, the standard ν_e survival probability over a baseline L in KamLAND reads:

$$P_{ee} = 1 - \frac{1}{2} \sin^2 2\theta_{12} \left(1 - \cos \left(\frac{\delta m^2 L}{2E} \right) \right). \quad (1)$$

In the presence of additional decoherence effects, the oscillating factor is exponentially suppressed, as shown in [11] for the atmospheric $\nu_\mu \rightarrow \nu_\mu$ channel. By changing the appropriate parameters for the KamLAND $\nu_e \rightarrow \nu_e$ channel, the results of [11] lead to the following modification of the previous equation,

$$P_{ee} = 1 - \frac{1}{2} \sin^2 2\theta_{12} \left(1 - e^{-\gamma L} \cos \left(\frac{\delta m^2 L}{2E} \right) \right), \quad (2)$$

where the dimensional parameter γ represents the inverse of the decoherence length after which the neutrino system gets mixed.¹ Equation (2) includes the limiting cases of pure oscillations ($\gamma = 0$ and $\delta m^2 \neq 0$) and of pure decoherence ($\gamma \neq 0$ and $\delta m^2 = 0$).

Unfortunately, lacking a fundamental theory for quantum gravity, the dependence of γ on the underlying dynamical and kinematical parameters (most notably the neutrino energy E) is unknown. Following common practice, such ignorance is parameterized in a power-law form

$$\gamma = \gamma_0 \left(\frac{E}{E_0} \right)^n, \quad (3)$$

where E_0 is an arbitrary pivot energy scale, which we set as $E_0 = 1$ GeV in order to facilitate the comparison with limits on γ -parameters investigated in other contexts (as reviewed, e.g., in [49]). We shall consider only five possible integer exponents,

$$n = 0, \pm 1, \pm 2, \quad (4)$$

which include the following cases of interest: The “energy independent” case ($n = 0$); the “Lorentz invariant” case [11] ($n = -1$); the case $n = +2$ that can arise in some D-brane or quantum-gravity models, in which $\gamma_0 \sim O(E_0^2/M_{\text{Planck}}) \sim 10^{-19}$ GeV is expected (see, e.g. [50]); and the case where decoherence might be induced by “matter density fluctuations” rather than by quantum gravity ($n = -2$, see Sec. V).

As previously remarked, the KamLAND collaboration [43] (see also [51]) has ruled out pure decoherence in the Lorentz invariant case ($n = -1$). In our statistical χ^2 analysis, we also find that this case is rejected at 3.6σ (i.e., $\Delta\chi^2 = 13$ with respect to pure oscillations). In addition, we find that the other exponents in Eq. (4) are also rejected at $> 3\sigma$ for the pure decoherence case. Therefore, decoherence effects can only be subdominant in KamLAND, namely

$$\gamma L \ll 1. \quad (5)$$

¹ Units: $[\gamma] = 1/\text{length} = \text{energy}$. Conversion factor: $(1 \text{ km})^{-1} = 1.97 \times 10^{-19} \text{ GeV}$.

For typical KamLAND neutrino energies ($E \sim \text{few MeV}$) and baselines ($L \sim 2 \times 10^2 \text{ km}$), the above inequality implies upper bounds on γ_0 , which range from $\gamma_0 \ll 10^{-26} \text{ GeV}$ ($n = -2$) to $\gamma_0 \ll 10^{-16} \text{ GeV}$ ($n = +2$). We do not refine the analysis of such bounds (placed by KamLAND alone), since they are superseded by solar data constraints, as shown in the next Section.

III. OSCILLATIONS WITH(OUT) DECOHERENCE EFFECTS IN SOLAR NEUTRINOS

The survival probability describing standard adiabatic ν_e transitions in the solar matter is given by the simple formula (up to small Earth matter effects)

$$P_{ee}^\odot = \frac{1}{2} \left(1 + \cos 2\tilde{\theta}_{12}(r_0) \cos 2\theta_{12} \right), \quad (6)$$

where $\tilde{\theta}_{12}(r_0)$ is the energy-dependent effective mixing angle in matter at the production radius r_0 (see, e.g., [52] and references therein).

In the presence of non-standard decoherence effects, we find that the energy dependent term is modulated by an exponential factor,

$$P_{ee}^\odot = \frac{1}{2} \left(1 + e^{-\gamma_\odot R_\odot} \cos 2\tilde{\theta}_{12}(r_0) \cos 2\theta_{12} \right), \quad (7)$$

where $R_\odot = 6.96 \times 10^5 \text{ km}$ is the Sun radius, while γ_\odot is defined as

$$\gamma_\odot = \gamma_0 g_n(E), \quad (8)$$

where the dimensionless function $g_n(E)$ embeds, besides the power-law dependence E^n , also the information about the solar density profile [which is instead absent in Eq. (6)]. The reader is referred to the Appendix for a derivation of Eq. (7) and for details about the function $g_n(E)$.

Equation (7) includes the subcase of pure oscillations ($\gamma_0 = 0$ and $\delta m^2 \neq 0$), but not the subcase of pure decoherence ($\gamma_0 \neq 0$ and $\delta m^2 = 0$), since the limit $\delta m^2 \rightarrow 0$ would entail strongly nonadiabatic transitions, and thus a breakdown of the adiabatic approximation assumed above. However, as noted in the previous section, the KamLAND data exclude the limit $\delta m^2 \rightarrow 0$; moreover, they require δm^2 values which are high enough to guarantee the validity of the adiabatic approximations, with or without subleading decoherence effects (as we have numerically verified). Therefore, for solar neutrinos, the only phenomenologically relevant cases are those including oscillations plus decoherence.²

We have analyzed all the available solar neutrino data with $(\delta m^2, \theta_{12}, \gamma_0)$ taken as free parameters. It turns out that, despite the allowance for an extra degree of freedom (γ_0), the data always prefer the pure oscillations ($\gamma_0 = 0$) as best fit, independently of the power-law index in Eq. (4). Since there are no indications in favor of decoherence effects, the exponent in Eq. (7) is expected to be small,

$$\gamma_\odot R_\odot \ll 1. \quad (9)$$

² For the sake of curiosity, we have anyway calculated P_{ee}^\odot for the pure decoherence case, by numerically solving the neutrino evolution equations (discussed in the Appendix) for $\delta m^2 = 0$ and $\gamma \neq 0$. We always find $P_{ee}^\odot > 1/2$, which is forbidden by ⁸B solar neutrino data [46].

TABLE I: Upper limits on the decoherence parameter γ_0 obtained for different values of n from a global fit to solar and KamLAND data, after marginalization of the mass-mixing parameters. The limits refer to 95% C.L. (i.e., 2σ , or $\Delta\chi^2 = 4$).

n	γ_0 (GeV)
-2	$< 0.81 \times 10^{-28}$
-1	$< 0.78 \times 10^{-26}$
0	$< 0.67 \times 10^{-24}$
+1	$< 0.58 \times 10^{-22}$
+2	$< 0.47 \times 10^{-20}$

For typical solar neutrino energies $E \sim 10$ MeV, it turns out that $g_n(E) \sim 0.2 \times 10^{-2n}$ (see the Appendix), and the above inequality can be translated into upper bounds on γ_0 , which range from $\gamma_0 \ll 10^{-28}$ GeV (for $n = -2$) to $\gamma_0 \ll 10^{-20}$ GeV (for $n = +2$). Such bounds are two to four orders of magnitude stronger than those placed by KamLAND alone (see the end of the previous Section). A useful complementarity then emerges between solar and KamLAND data in joint fits: The former dominate the constraints on decoherence effects, while the latter fix the mass-mixing parameters independently of (negligible) decoherence effects.

IV. COMBINATION OF SOLAR AND KAMLAND DATA: RESULTS AND DISCUSSION

We have performed a joint analysis of solar and KamLAND data³ in the $(\delta m^2, \sin^2 \theta_{12}, \gamma_0)$ parameter space for the five power-law exponents $n = 0, \pm 1, \pm 2$. The main results are: (i) $\gamma_0 = 0$ is always preferred at best fit, i.e., there is no indication in favor of decoherence effects; (ii) the best fit values and the marginalized bounds for $(\delta m^2, \sin^2 \theta_{12})$ do not appreciably change from those obtained in the pure oscillation case, namely, $\delta m^2 = (7.92 \pm 0.71) \times 10^{-5}$ eV² and $\sin^2 \theta_{12} = (0.314_{-0.047}^{+0.057})$ at $\pm 2\sigma$ [44]; (iii) significant upper bounds can be set on the decoherence parameter γ_0 . Our limits on γ_0 are given numerically in Table I (at the 2σ level, $\Delta\chi^2 = 4$) and graphically in Fig. 1 (at 2σ and 3σ level). Such limits are consistent with those discussed qualitatively after Eq. (9) in the previous Section.

Figure 1 clearly shows that the bounds on γ_0 scale with n almost exactly as a power law, changing by about two decades for $|\Delta n| = 1$. The reason is that the bounds are dominated by solar neutrino data, and in particular by data probing the ⁸B neutrinos in a relatively narrow energy range around $E \sim 10$ MeV; the power-law dependence assumed in Eq. (3) and embedded in the function $g_n(E)$ then implies that the parameter γ_0 scales roughly as $(E/E_0)^{-n} \sim 10^{2n}$.

Although the case of no decoherence ($\gamma_0 = 0$) is preferred, it makes sense to ask what one should observe for decoherence effects as large as currently allowed by the data at, say, the 2σ level. Figure 2 compares the P_{ee}^\odot energy profile for the cases of pure oscillations (left

³ The details of the data set, of the solar model used [53] and of the statistical χ^2 analysis have been reported in [44] and are not repeated here.

panel) and of oscillations plus decoherence (right panel), where γ_0 is taken equal to the upper bound at 2σ , as taken from Table I.⁴ It can be seen that decoherence effects, to some extent, mimic the effects of a larger mixing. For instance, the curve with $n = 0$ in the right panel is not much different from the curve at $\sin^2 \theta_{12} = 0.371$ (upper 2σ value) in the left panel. As a consequence, one expects some degeneracy between the parameters γ_0 and $\sin^2 \theta_{12}$ when fitting the data. The degeneracy is only partial however, because decoherence effects can significantly change both the shape and the slope of the energy profile within the current 2σ bounds, as evident in the right panel. Therefore, future measurements of the (currently not well constrained) solar neutrino energy spectrum will provide further important probes of decoherence effects.

The variation of P_{ee}^\odot due to subdominant decoherence effects [see Eqs. (6) and (7)] is given, in first approximation, by

$$\Delta P_{ee}^\odot \simeq -\frac{1}{2} \gamma_\odot R_\odot \cos 2\tilde{\theta}_{12} \cos 2\theta_{12} , \quad (10)$$

and changes sign with $\cos 2\tilde{\theta}_{12}$. As the energy increases, the value of $\cos 2\tilde{\theta}_{12}$ changes from $\cos \theta_{12} > 0$ (low-energy, vacuum-dominated regime) to -1 (high-energy, matter-dominated regime), the transition being located around 2 MeV for the ^8B neutrino curves shown in Fig. 2. This fact explains the general increase of P_{ee}^\odot for $E \gtrsim 2$ MeV in the right panel of Fig. 2. More detailed features depend instead on the energy behavior of the function $g_n(E)$, which modulates decoherence effects (see the Appendix). In general, $g_n(E)$ grows rapidly with increasing energy for $n > 0$ (which explains the high-energy upturn of the curves with $n = +1$ and $n = +2$), while it vanishes with decreasing energy for all $n \neq -2$ (which explains the low-energy equality of all curves but for $n = -2$).⁵ The “bunching” of the curves around $E \sim 10$ MeV in the right panel of Fig. 2 is in part a data selection effect, since this energy region is strongly constrained by precise ^8B neutrino data. Further spectral ^8B data will be very useful to constrain the slope of the energy spectrum and thus also the sign of the power-law index n .

Figure 3 illustrates the partial degeneracy between decoherence effects and mixing angle, as a shift in the allowed regions for fixed $\gamma_0 \neq 0$ in three representative cases (from left to right, $n = -2, 0, +2$). In each panel, the thin dotted curves enclose the mass-mixing parameter regions allowed at 2σ by the standard oscillation fit of solar data (larger region) and by solar plus KamLAND data (smaller region). The thick solid curves refer to the same data, but fixing *a priori* the decoherence parameter γ_0 at the 2σ upper limit value in Table I. In all cases in Fig. 3, the curves with $\gamma_0 \neq 0$ are shifted to lower values of the mixing angle, as compared to pure oscillations; this means that decoherence effects can be partly traded for a smaller value of the mixing angle in solar neutrino oscillations. Therefore, should future solar neutrino data prefer smaller (larger) values of $\sin^2 \theta_{12}$ with respect to KamLAND data, there would be more (less) room for possible subdominant decoherence effects. As already remarked, the degeneracy between γ_0 and $\sin^2 \theta_{12}$ is only partial, and future neutrino spectroscopy will provide a further handle to break it, should decoherence effects (if any) be found.

⁴ For definiteness, Fig. 2 shows the daytime probability of ^8B neutrinos, averaged over their production region in the Sun.

⁵ Constraints on the specific case $n = -2$ might thus benefit of sub-MeV solar neutrino observations in Borexino [54].

We conclude this section by confronting the bounds in Table I with those derivable from the analysis of atmospheric neutrino data (which, by themselves, exclude pure decoherence, at least in the $n = -1$ case [55]). In principle, a direct comparison is not possible, since the γ_0 parameter introduced here for the solar $\nu_e \rightarrow \nu_e$ channel does not need to be the same as for the atmospheric $\nu_\mu \rightarrow \nu_\mu$ channel. However, if the γ_0 's for these two channels are *assumed* to be roughly equal in size, then it is easy to realize that solar+KamLAND neutrinos set stronger (weaker) bounds than atmospheric neutrinos for $n < 0$ ($n > 0$), as a consequence of the different neutrino energy range probed. In fact, due to the assumed power-law energy dependence of decoherence effects, negative (positive) values of n are best probed by low-energy solar (high-energy atmospheric) neutrino experiments. For the intermediate case ($n = 0$), it turns out that matter effects render solar neutrinos more sensitive to γ_0 than atmospheric neutrinos. Just to make specific numerical examples: for $n = (-1, 0, +2)$ one roughly gets the bounds $\gamma_0 \lesssim (0.7 \times 10^{-21}, 0.4 \times 10^{-22}, 0.9 \times 10^{-27})$ GeV from atmospheric [11] (plus accelerator [12]) neutrino data, to be compared with the corresponding limits from solar+KamLAND data from Table I, $\gamma_0 < (0.78 \times 10^{-26}, 0.67 \times 10^{-24}, 0.47 \times 10^{-20})$ GeV. Solar neutrinos clearly win over atmospheric neutrinos for $n \leq 0$. This comparison must be taken with a grain of salt, since it can radically change by assuming either independent γ_0 's in different oscillation channels, or functional forms of $\gamma(E)$ different from power laws.

Finally we observe that in the $n = +2$ case, motivated by some “quantum-gravity” or “string-inspired” models [50], the solar+KamLAND limit on γ_0 is one order of magnitude lower than the theoretical expectation [$\gamma_0 \sim O(E_0^2/M_{\text{Planck}}) \sim 10^{-19}$ GeV]. In the case of atmospheric neutrinos, this bound is even stronger ($\gamma_0 < 0.9 \times 10^{-27}$ GeV). Consequently, these models appear strongly disfavored, at least in the neutrino sector.

V. RECOVERING THE CASE OF DENSITY FLUCTUATIONS IN THE SUN

Decoherence effects in solar neutrino oscillations can be induced not only by quantum gravity, but also by more “prosaic” sources, such as matter density fluctuations—possibly induced by turbulence in the innermost regions of the Sun. This topic has been widely investigated in the literature [56, 57, 58, 59, 60, 61, 62, 63, 64, 65], and quantitative upper limits have already been set [61, 62, 63, 64] by combining solar data and first KamLAND results.

It turns out that stochastic density fluctuations lead (with appropriate redefinition of parameters) to effects which have the same functional form as those induced by quantum gravity in the $n = -2$ case. More precisely, let us consider fluctuations of the solar electron density N_e around the average value $\langle N_e \rangle$ predicted by the standard solar model,

$$N_e(r) = (1 + \beta F(r)) \langle N_e(r) \rangle, \quad (11)$$

where $F(r)$ is a random variable describing fluctuations at a given radius r , and β represents their fractional amplitude around the average. It is customary to assume a delta-correlated (white) noise,

$$\langle F(r_1) F(r_2) \rangle = 2\tau \delta(r_1 - r_2), \quad (12)$$

where τ is the correlation length of fluctuations along the (\sim radial) neutrino direction.

As shown in [59] through a perturbative method (which inspired our approach to decoherence in the Appendix), the effect of delta-correlated noise on adiabatic neutrino flavor

transitions can be embedded through an exponential damping factor as in Eq. (7). The functional form turns out to be the same as for the $n = -2$ case, provided that one makes—in our notation—the replacement

$$\gamma_0 \rightarrow \beta^2 \tau \left(\frac{\delta m^2}{2E_0} \right)^2. \quad (13)$$

By using the bound $\gamma_0 < 0.81 \times 10^{-28}$ GeV (Table I, case $n = -2$) and the best-fit value $\delta m^2 = 7.92 \times 10^{-5}$ eV², one gets the following upper limit

$$\beta^2 \tau < 1.02 \times 10^{-2} \text{ km } (2\sigma), \quad (14)$$

on the parameter combination $\beta^2 \tau$ which is relevant [59, 63] for density fluctuation effects on neutrino propagation.

As stressed in [63], care must be taken in extracting an upper limit on the fractional amplitude β for fixed correlation length τ . Indeed, the delta-correlated noise is an acceptable approximation only if the correlation length τ is much smaller than the oscillation wavelength in matter—a condition that becomes critical for low neutrino energies. In particular, assuming a reference value $\tau = 10$ km as in [63], such condition is violated for energies $E \lesssim 1$ MeV. Following [63], we have thus excluded low-energy, radiochemical solar neutrino data from the solar+KamLAND data fit, and obtained a slightly weaker (but more reliable) upper bound from the analysis of ⁸B neutrino data only,

$$\beta^2 \tau < 1.16 \times 10^{-2} \text{ km } (2\sigma), \quad (15)$$

which, for $\tau = 10$ km, translates into an upper limit on the fractional fluctuation amplitude,

$$\beta < 3.4\% (2\sigma). \quad (16)$$

This limit improves the previous one derived in [63] ($\beta < 6.3\%$ at 2σ) by a factor of ~ 2 , essentially as a result of the inclusion of the most recent solar and KamLAND neutrino data appeared after [63].⁶

VI. SUMMARY AND CONCLUSIONS

In this paper, we have investigated hypothetical decoherence effects (e.g., induced by quantum gravity) in the $\nu_e \rightarrow \nu_e$ oscillation channel explored by the solar and KamLAND experiments. In both kinds of experiments, decoherence effects can be embedded through exponential damping factors, proportional to a common parameter γ_0 , which modulate the energy-dependent part of the ν_e survival probability. By assuming that the (unknown) functional form of decoherence effects is a power-law in energy (E^n), we have studied the phenomenological constraints on the main decoherence parameter (γ_0) for $n = 0, \pm 1, \pm 2$. It turns out that both solar and KamLAND data do not provide indications in favor of decoherence effects and prefer the standard oscillation case ($\gamma_0 = 0$) for any index n . By combining the two data sets, n -dependent upper bounds (dominated by solar neutrino data)

⁶ We have verified that, by adopting the same (older) data set and standard solar model as used in [63], we recover the same 2σ upper limit, $\beta \lesssim 6\%$.

have been derived on γ_0 , as reported in Table I and shown in Fig. 1. In the “Lorentz-invariant” case $n = -1$, we obtain the upper limit $\gamma_0 < 0.78 \times 10^{-26}$ GeV at 95% C.L. For $n = -2$, the results can also be interpreted as limits on the amplitude of possible (delta-correlated) density fluctuations in the Sun, which we improve by a factor of two [Eqs. (15) and (16)] with respect to previous bounds.

Further progress might come from a better determination of the energy profile of solar neutrino flavor transitions as well as from more precise measurements of $\sin^2 \theta_{12}$ (which is partly degenerate with γ_0), attainable with KamLAND and future long-baseline reactor neutrino experiments [66].

APPENDIX: DECOHERENCE AND MATTER EFFECTS IN SOLAR NEUTRINOS

In this section we discuss a perturbative calculation of decoherence effects for solar neutrinos, where matter effects are known to be relevant. The approach, inspired by the work [59], draws on the formalism and the notation introduced in [11] for the case of decoherence in the $\nu_\mu \rightarrow \nu_\mu$ channel, here adapted to the $\nu_e \rightarrow \nu_e$ channel. In the following, the notation is made more compact by setting $\theta = \theta_{12}$, $c_{2\theta} = \cos 2\theta_{12}$, $s_{2\theta} = \sin 2\theta_{12}$, $P_{ee} = P_{ee}^\odot$ etc.

Decoherence effects in the flavor evolution of the (ν_e, ν_a) system (where $a = \mu, \tau$) along the space coordinate $r (\simeq t)^7$ can be described in terms of the neutrino density matrix, obeying a modified master equation of the form [67]

$$\frac{d\rho}{dr} = -i[H_v + H_m(r), \rho] - \gamma[D, [D, \rho]] , \quad (17)$$

where H_v (H_m) is the “vacuum” (matter) Hamiltonian, and the operator D embeds decoherence effects with amplitude γ , parameterized as in Eq. (3): $\gamma = \gamma_0(E/E_0)^n$ with $E_0 = 1$ GeV. While unitarity is preserved (i.e., $\text{Tr}\rho(r) = 1$), coherence is lost in the propagation ($\frac{d}{dr}\text{Tr}\rho^2 \leq 0$). Equation (17) satisfies the conditions of complete positivity [68] and non-decreasing entropy in the ν system evolution [69].

In the flavor basis the standard oscillation terms read

$$H_v = -\frac{k}{2}U_\theta\sigma_3U_\theta^\dagger = \frac{k}{2}\begin{bmatrix} -c_{2\theta} & s_{2\theta} \\ s_{2\theta} & c_{2\theta} \end{bmatrix} , \quad (18)$$

$$H_m = -\frac{V(r)}{2}\sigma_3 , \quad (19)$$

where σ_3 is the third Pauli matrix, $k = \delta m^2/2E$ is the vacuum wavenumber, and $V(r) = \sqrt{2}G_F N_e(r)$ is the interaction potential in matter.

As in [11], we assume energy conservation for evolution in vacuum, i.e., $\text{Tr}[H_v\rho(r)] = \text{constant}$. This condition is satisfied if $[H_v, D] = 0$ [4, 70], namely, in a two-dimensional system, if $D \propto H_v$. We can thus take

$$D_\theta = \frac{1}{2}\begin{bmatrix} -c_{2\theta} & s_{2\theta} \\ s_{2\theta} & c_{2\theta} \end{bmatrix} , \quad (20)$$

⁷ Note that r does not necessarily coincide with the radial coordinate, due to the extended neutrino production region (which is taken into account in our analysis.)

without loss of generality, since any overall factor can be absorbed in γ_0 . We also make the plausible assumption that Eq. (20) is not altered for evolution in matter, since decoherence induced by quantum gravity is unrelated to electroweak matter effects.

As usual, Eq. (17) can be written in terms of a “polarization” vector \mathbf{P} with components $P_i = \frac{1}{2}\text{Tr}[\rho\sigma_i]$ (Bloch equation):

$$\begin{aligned}\frac{d\mathbf{P}}{dr} &= [k\mathbf{n} + V(r)\mathbf{e}_3] \times \mathbf{P} - \gamma\mathbf{P}_\perp \\ &= \mathcal{H}(r)\mathbf{P} - \gamma\mathcal{D}_\theta\mathbf{P}\end{aligned}\quad (21)$$

where $\mathbf{n} = [s_{2\theta}, 0, -c_{2\theta}]^T$, $\mathbf{P}_\perp = \mathbf{P} - (\mathbf{P} \cdot \mathbf{n})\mathbf{n}$, and:

$$\mathcal{H}(r) = \begin{bmatrix} 0 & -V(r) + kc_{2\theta} & 0 \\ V(r) - kc_{2\theta} & 0 & -ks_{2\theta} \\ 0 & ks_{2\theta} & 0 \end{bmatrix}, \quad (22)$$

$$\mathcal{D}_\theta = \begin{bmatrix} c_{2\theta}^2 & 0 & c_{2\theta}s_{2\theta} \\ 0 & 1 & 0 \\ c_{2\theta}s_{2\theta} & 0 & s_{2\theta}^2 \end{bmatrix}. \quad (23)$$

Note that for $V = 0$ (vacuum propagation), the solution of the above Bloch equation leads to the survival probability in Eq. (2), (see [11] for details.)

The matrix \mathcal{H} has eigenvalues $\lambda_0 = 0$ and $\lambda_\pm = \pm\tilde{k}$, corresponding to the eigenvectors:

$$\mathbf{u}_0 = \begin{bmatrix} s_{2\tilde{\theta}} \\ 0 \\ -c_{2\tilde{\theta}} \end{bmatrix}, \quad \mathbf{u}_\pm = \frac{1}{\sqrt{2}} \begin{bmatrix} c_{2\tilde{\theta}} \\ \pm i \\ s_{2\tilde{\theta}} \end{bmatrix}. \quad (24)$$

In the above equations, a “tilde” marks effective parameters in matter: \tilde{k} is the oscillation wavenumber in matter, defined through $\tilde{k}/k = [1 - 2Vc_{2\theta}/k + (V/k)^2]^{1/2}$, while $\tilde{\theta}$ is the mixing angle in matter, defined through $s_{2\tilde{\theta}} = ks_{2\theta}/\tilde{k}$ and $c_{2\tilde{\theta}} = (kc_{2\theta} - V)/\tilde{k}$. The matrix \mathcal{H} is diagonalized through the matrix $\mathcal{R}(\tilde{\theta}) = [\mathbf{u}_0, \mathbf{u}_+, \mathbf{u}_-]$: $\mathcal{R}^\dagger(\tilde{\theta}) \cdot \mathcal{H} \cdot \mathcal{R}(\tilde{\theta}) = \text{diag}[0, +i\tilde{k}, -i\tilde{k}]$.

In the absence of decoherence effects, the adiabatic solution of Eq. (21) appropriate for current solar neutrino phenomenology is

$$\mathbf{P}(R_\odot) = \mathcal{R}(\theta) \cdot \text{diag} \left[1, e^{+i \int_{r_0}^{R_\odot} dr \tilde{k}(r)}, e^{-i \int_{r_0}^{R_\odot} dr \tilde{k}(r)} \right] \cdot \mathcal{R}^\dagger(\tilde{\theta}_0) \mathbf{P}(r_0) \quad (25)$$

where $\mathbf{P}(r_0) = {}^T[0, 0, 1]$ for an initial ν_e state, $\tilde{\theta}_0$ is the mixing angle in matter at the production point r_0 , and $\tilde{\theta} = \theta$ is taken at $r = R_\odot$. After averaging on the fast oscillating terms (a “standard” decoherence effect), one recovers the usual adiabatic formula [Eq. (6)] for the survival probability P_{ee}

$$P_{ee} = \text{Tr} [\rho|\nu_e\rangle\langle\nu_e|] = \frac{1 + P_3(R_\odot)}{2} = \frac{1 + c_{2\theta}c_{2\tilde{\theta}_0}}{2}. \quad (26)$$

Let us now treat the term $-\gamma\mathcal{D}_\theta\mathbf{P}$ in Eq. (21) as a perturbation [59]. The corrections to the eigenvectors lead to variations of P_{ee} of $O(\gamma/k) \lesssim 10^{-3}$ (for the range of γ/k allowed a

posteriori by the fit to solar neutrino data) and can be neglected. The corrections to the two eigenvalues λ_{\pm} can also be neglected, since they would only lead to a further damping of the fast oscillating terms, which are already averaged out.⁸

The first-order correction to the eigenvalue λ_0 (whose unperturbed value is zero) is the only relevant one,

$$\delta\lambda_0 = -\gamma \mathbf{u}_0^\dagger \mathcal{D}_\theta \mathbf{u}_0 = -\gamma \sin^2 2(\tilde{\theta} - \theta) . \quad (27)$$

and leads to the following correction to Eq. (26):

$$P_{ee} = \frac{1 + e^{-\Gamma} c_{2\theta} c_{2\tilde{\theta}_0}}{2} , \quad (28)$$

where

$$\Gamma = \gamma \int_{r_0}^{R_\odot} \left[\frac{V(r) s_{2\tilde{\theta}}(r)}{k} \right]^2 dr . \quad (29)$$

Equation (7) is then recovered by setting $\gamma_\odot = \gamma_0 g_n(E)$ and by defining the dimensionless function $g_n(E)$ as

$$g_n(E) = \left(\frac{E}{E_0} \right)^n \int_{r_0}^{R_\odot} \left[\frac{V(r) s_{2\tilde{\theta}}(r)}{k} \right]^2 \frac{dr}{R_\odot} . \quad (30)$$

The function $g_n(E)$ depends mostly on the neutrino energy E and, to some extent, on the parameters r_0 , δm^2 , and $\sin^2 \theta_{12}$. Figure 4 shows this function as calculated for $r_0 = 0$, $\delta m^2 = 7.92 \times 10^{-5} \text{ eV}^2$, and $\sin^2 \theta_{12} = 0.314$. For $E \rightarrow 0$ the function $g_n(E)$ (and the associated decoherence effect) vanishes, except for the case $n = -2$, where the factors E^{-2} and k^{-2} cancel out and provide a finite limit $g_{-2}(0) \neq 0$.

We have tested the analytical Eq. (28) against the results of a numerical integration of the Bloch equation, for many representative points in the parameter space relevant for solar ν phenomenology, and we find very good agreement ($\delta P_{ee} < 10^{-4}$) for all values of $n \neq -2$. Only in the case $n = -2$, the comparison of analytical and numerical results is slightly worse (but still very good, $\delta P_{ee} < 10^{-3}$) at the lowest detectable energies ($\sim 0.1 \text{ MeV}$), due to the breakdown of perturbation theory for $E \rightarrow 0$. For practical purposes, however, the modified adiabatic Eq. (28) accurately replaces the results of numerical solutions of the Bloch equation for solar neutrinos.

Acknowledgments

The work of G.L. Fogli, E. Lisi, A. Marrone, and D. Montanino is supported by the Italian MUR and INFN through the ‘‘Astroparticle Physics’’ research project. The work of A. Palazzo is supported by INFN.

[1] S.W. Hawking, Commun. Math. Phys. **43**, 199 (1975); *ibidem* **87**, 395 (1982); Phys. Rev. D **14**, 2460 (1976).

⁸ Similarly, non-standard decoherence effects in the path from the Sun surface to the Earth are irrelevant, since they would simply damp the (already averaged out) fast oscillations. The only relevant effects occur within the Sun, through the modification of the standard evolution in matter.

- [2] S.B. Giddings and A. Strominger, Nucl. Phys. B **307**, 854 (1988); W.H. Zurek, Physics Today **44**, No. 10, p. 36 (1991); G. Amelino-Camelia, J. Ellis, N.E. Mavromatos, and D.V. Nanopoulos, Int. J. Mod. Phys. A **12**, 607 (1997); L.J. Garay, Int. J. Mod. Phys. A **14**, 4079 (1999).
- [3] J. Ellis, J.S. Hagelin, D.V. Nanopoulos, and M. Srednicki, Nucl. Phys. B **241**, 381 (1984).
- [4] T. Banks, L. Susskind, and M.E. Peskin, Nucl. Phys. B **244**, 125 (1984).
- [5] P. Huet and M.E. Peskin, Nucl. Phys. B **488**, 335 (1997); J. Ellis, J.L. Lopez, N.E. Mavromatos, and D.V. Nanopoulos, Phys. Rev. D **53**, 3846 (1996); F. Benatti and R. Floreanini, Phys. Lett. B **389**, 100 (1996); *ibidem* **401**, 337 (1997).
- [6] J. Bernabeu, N.E. Mavromatos, and S. Sarkar, Phys. Rev. D **74**, 045014 (2006).
- [7] F. Benatti and R. Floreanini, Phys. Lett. B **451**, 422 (1999).
- [8] Y. Liu, L. Hu, and M.L. Ge, Phys. Rev. D **56**, 6648 (1997).
- [9] Y. Liu, J.L. Chen, and M.L. Ge, J. Phys. G **24**, 2289 (1998); C.P. Sun and D.L. Zhou, hep-ph/9808334.
- [10] C.H. Chang, W.S. Dai, X.Q. Li, Y. Liu, F.C. Ma, and Z.J. Tao, Phys. Rev. D **60**, 033006 (1999).
- [11] E. Lisi, A. Marrone, and D. Montanino, Phys. Rev. Lett. **85**, 1166 (2000).
- [12] G. L. Fogli, E. Lisi, A. Marrone, and D. Montanino, Phys. Rev. D **67**, 093006 (2003).
- [13] A. M. Gago, E.M. Santos, W.J.C. Teves, and R. Zukanovich Funchal, Phys. Rev. D **63**, 073001 (2001).
- [14] M. Blennow, T. Ohlsson, and W. Winter, JHEP **0506**, 049 (2005); Eur. Phys. J. C **49**, 1023 (2007).
- [15] Super-Kamiokande Collaboration, Y. Fukuda *et al.*, Phys. Rev. Lett. **81**, 1562 (1998).
- [16] D.V. Ahluwalia, Mod. Phys. Lett. A **16**, 917 (2001).
- [17] D. Hooper, D. Morgan, and E. Winstanley, Phys. Lett. B **609**, 206 (2005).
- [18] D. Hooper, D. Morgan, and E. Winstanley, Phys. Rev. D **72**, 065009 (2005).
- [19] L.A. Anchordoqui, H. Goldberg, M.C. Gonzalez-Garcia, F. Halzen, D. Hooper, S. Sarkar and T.J. Weiler, Phys. Rev. D **72**, 065019 (2005).
- [20] D. Morgan, E. Winstanley, J. Brunner, and L.F. Thompson, Astropart. Phys. **25**, 311 (2006).
- [21] F. Benatti and R. Floreanini, JHEP **0002**, 032 (2000).
- [22] F. Benatti and R. Floreanini, Phys. Rev. D **64**, 085015 (2001).
- [23] G. Barenboim and N.E. Mavromatos, JHEP **0501**, 034 (2005).
- [24] G. Barenboim, N.E. Mavromatos, S. Sarkar, and A. Waldron-Lauda, Nucl. Phys. B **758**, 90 (2006).
- [25] G. Barenboim and N.E. Mavromatos, Phys. Rev. D **70**, 093015 (2004).
- [26] N.E. Mavromatos and S. Sarkar, Phys. Rev. D **72**, 065016 (2005).
- [27] S. Sarkar, hep-ph/0610010.
- [28] Z. Maki, M. Nakagawa, and S. Sakata, Prog. Theor. Phys. **28**, 870 (1962); B. Pontecorvo, Zh. Eksp. Teor. Fiz. **53**, 1717 (1967) [Sov. Phys. JETP **26**, 984 (1968)].
- [29] L. Wolfenstein, Phys. Rev. D **17**, 2369 (1978); S.P. Mikheev and A.Yu. Smirnov, Yad. Fiz. **42**, 1441 (1985) [Sov. J. Nucl. Phys. **42**, 913 (1985)].
- [30] L. Wolfenstein, in *Neutrino '78*, 8th International Conference on Neutrino Physics and Astrophysics (Purdue U., West Lafayette, Indiana, 1978), ed. by E.C. Fowler (Purdue U. Press, 1978), p. C3.
- [31] Homestake Collaboration, B.T. Cleveland, T. Daily, R. Davis Jr., J.R. Distel, K. Lande, C.K. Lee, P.S. Wildenhain, and J. Ullman, Astrophys. J. **496**, 505 (1998).

- [32] Kamiokande Collaboration, Y. Fukuda *et al.*, Phys. Rev. Lett. **77**, 1683 (1996).
- [33] SAGE Collaboration, J.N. Abdurashitov *et al.*, J. Exp. Theor. Phys. **95**, 181 (2002) [Zh. Eksp. Teor. Fiz. **95**, 211 (2002)].
- [34] GALLEX Collaboration, W. Hampel *et al.*, Phys. Lett. B **447**, 127 (1999).
- [35] Gallium Neutrino Observatory (GNO) Collaboration, M. Altmann *et al.*, Phys. Lett. B **616**, 174 (2005).
- [36] V. Gavrin, talk at *Neutrino 2006*, XXII International Conference on Neutrino Physics and Astrophysics (Santa Fe, New Mexico, USA, 2006). Website: neutrinosantafe06.com
- [37] SK Collaboration, S. Fukuda *et al.*, Phys. Rev. Lett. **86**, 5651 (2001); Phys. Rev. Lett. **86**, 5656 (2001); Phys. Lett. B **539**, 179 (2002).
- [38] SK Collaboration, M.B. Smy *et al.*, Phys. Rev. D **69**, 011104 (2004).
- [39] SNO Collaboration, Q.R. Ahmad *et al.*, Phys. Rev. Lett. **87**, 071301 (2001); Phys. Rev. Lett. **89**, 011301 (2002); Phys. Rev. Lett. **89**, 011302 (2002).
- [40] SNO Collaboration, S.N. Ahmed *et al.*, Phys. Rev. Lett. **92**, 181301 (2004).
- [41] SNO Collaboration, B. Aharmim *et al.*, Phys. Rev. C **72**, 055502 (2005).
- [42] KamLAND Collaboration, K. Eguchi *et al.*, Phys. Rev. Lett. **90**, 021802 (2003).
- [43] KamLAND Collaboration, T. Araki *et al.*, Phys. Rev. Lett. **94**, 081801 (2005).
- [44] G.L. Fogli, E. Lisi, A. Marrone, and A. Palazzo, Prog. Part. Nucl. Phys. **57**, 742 (2006).
- [45] M. Maltoni, T. Schwetz, M.A. Tortola and J.W.F. Valle, New J. Phys. **6**, 122 (2004) [arXiv:hep-ph/0405172].
- [46] G.L. Fogli, E. Lisi, A. Marrone, and A. Palazzo, Phys. Lett. B **583**, 149 (2004); G. Fogli and E. Lisi, New J. Phys. **6**, 139 (2004).
- [47] O.G. Miranda, M.A. Tortola and J.W.F. Valle, JHEP **0610**, 008 (2006).
- [48] Particle Data Group, W.M. Yao *et al.*, J. Phys. G **33**, 1 (2006).
- [49] L.A. Anchordoqui, J. Phys. Conf. Ser. **60**, 191 (2007); L. Anchordoqui and F. Halzen, Annals Phys. **321**, 2660 (2006).
- [50] J. Ellis, N.E. Mavromatos, D.V. Nanopoulos, and E. Winstanley, Mod. Phys. Lett. A **12**, 243 (1997); J.R. Ellis, N.E. Mavromatos, and D.V. Nanopoulos, Mod. Phys. Lett. A **12**, 1759 (1997); R. Gambini, R.A. Porto, and J. Pullin, Class. Quant. Grav. **21**, L51 (2004).
- [51] T. Schwetz, Phys. Lett. B **577**, 120 (2003).
- [52] A.Yu. Smirnov, in the Proceedings of IPM School and Conference on Lepton and Hadron Physics (IPM-LHP06), Teheran, Iran, 2006; hep-ph/0702061.
- [53] J.N. Bahcall, A.M. Serenelli and S. Basu, Astrophys. J. **621**, L85 (2005).
- [54] Borexino Collaboration, G. Alimonti *et al.* Astropart. Phys. **16**, 205 (2002).
- [55] Super-Kamiokande Collaboration, Y. Ashie *et al.*, Phys. Rev. Lett. **93**, 101801 (2004).
- [56] F.N. Loreti and A.B. Balantekin, Phys. Rev. D **50**, 4762 (1994).
- [57] H. Nunokawa, A. Rossi, V.B. Semikoz, and J.W.F. Valle, Nucl. Phys. B **472**, 495 (1996).
- [58] A.B. Balantekin, J.M. Fetter, and F.N. Loreti, Phys. Rev. D **54**, 3941 (1996).
- [59] C.P. Burgess and D. Michaud, Annals. Phys. **256**, 1 (1997).
- [60] A.A. Bykov, M.C. Gonzalez-Garcia, C. Pena-Garay, V.Y. Popov and V.B. Semikoz, hep-ph/0005244.
- [61] C.P. Burgess, N.S. Dzhililov, M. Maltoni, T.I. Rashba, V.B. Semikoz, M.A. Tortola and J.W.F. Valle, Astrophys. J. **588**, L65 (2003).
- [62] M.M. Guzzo, P.C. de Holanda, and N. Reggiani, Phys. Lett. B **569**, 45 (2003); N. Reggiani, M.M. Guzzo, and P.C. de Holanda, Braz. J. Phys. **34**, 1729 (2004).
- [63] A.B. Balantekin and H. Yüksel, Phys. Rev. D **68**, 013006 (2003).

- [64] C.P. Burgess, N.S. Dzhililov, M. Maltoni, T.I. Rashba, V.B. Semikoz, M.A. Tortola and J.W.F. Valle, JCAP **0401**, 007 (2004).
- [65] F. Benatti and R. Floreanini, Phys. Rev. D **71**, 013003 (2005).
- [66] S.T. Petcov and T. Schwetz, Phys. Lett. B **642**, 487 (2006).
- [67] G. Lindblad, Commun. Math. Phys. **48**, 119 (1976).
- [68] V. Gorini, A. Frigerio, M. Verri, A. Kossakowski, and E.C.G. Sudarshan, J. Math. Phys. (N.Y.) **17**, 821 (1976).
- [69] F. Benatti and H. Narnhofer, Lett. Math. Phys. **15**, 325 (1988).
- [70] J. Liu, Phys. Lett. B **314**, 52 (1993).

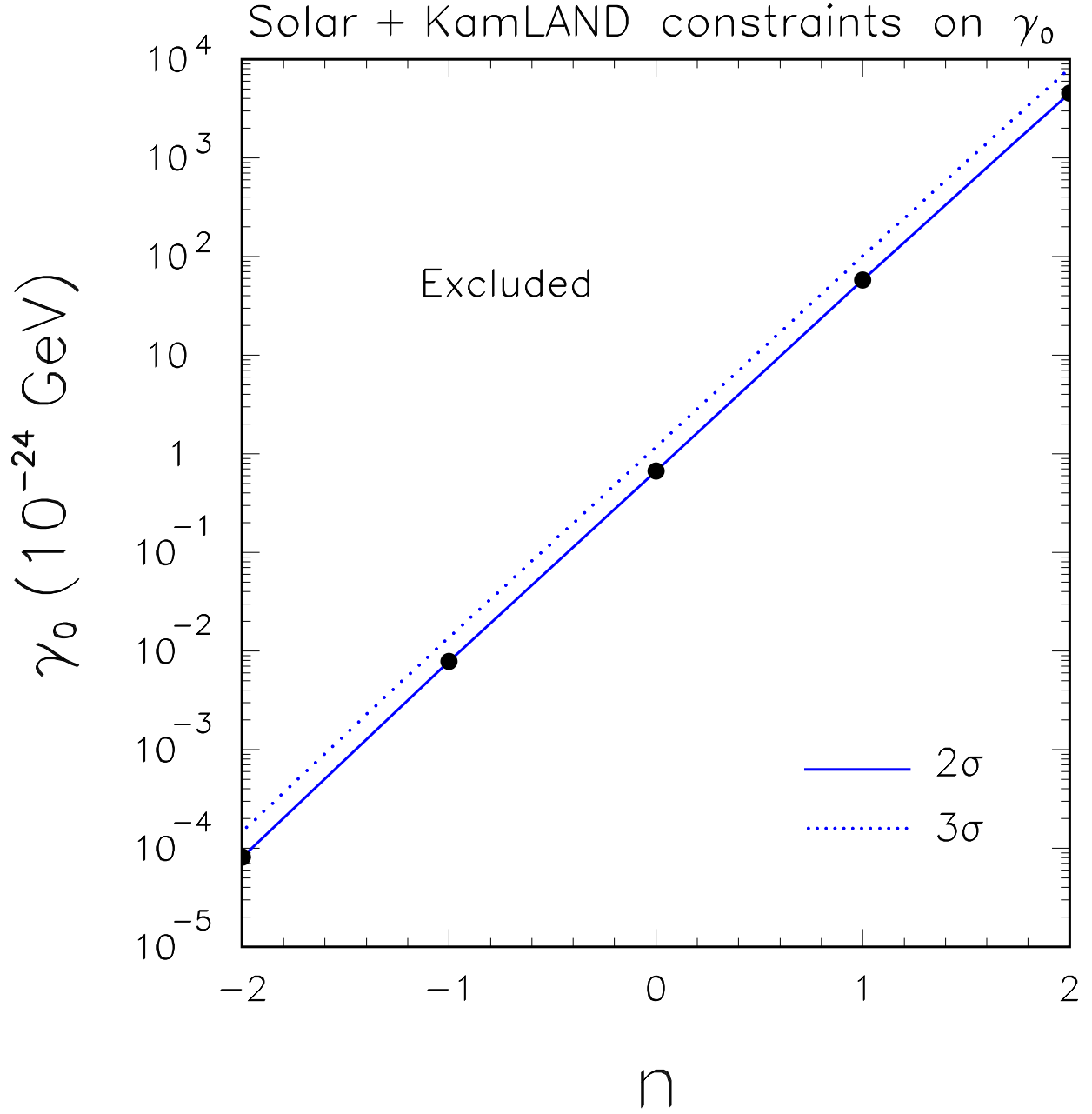


FIG. 1: Upper bounds on the decoherence parameter γ_0 as a function of the power-law index n , as obtained from a combined analysis of solar and KamLAND data. The solid and dotted curves refer to 2σ and 3σ confidence level, respectively.

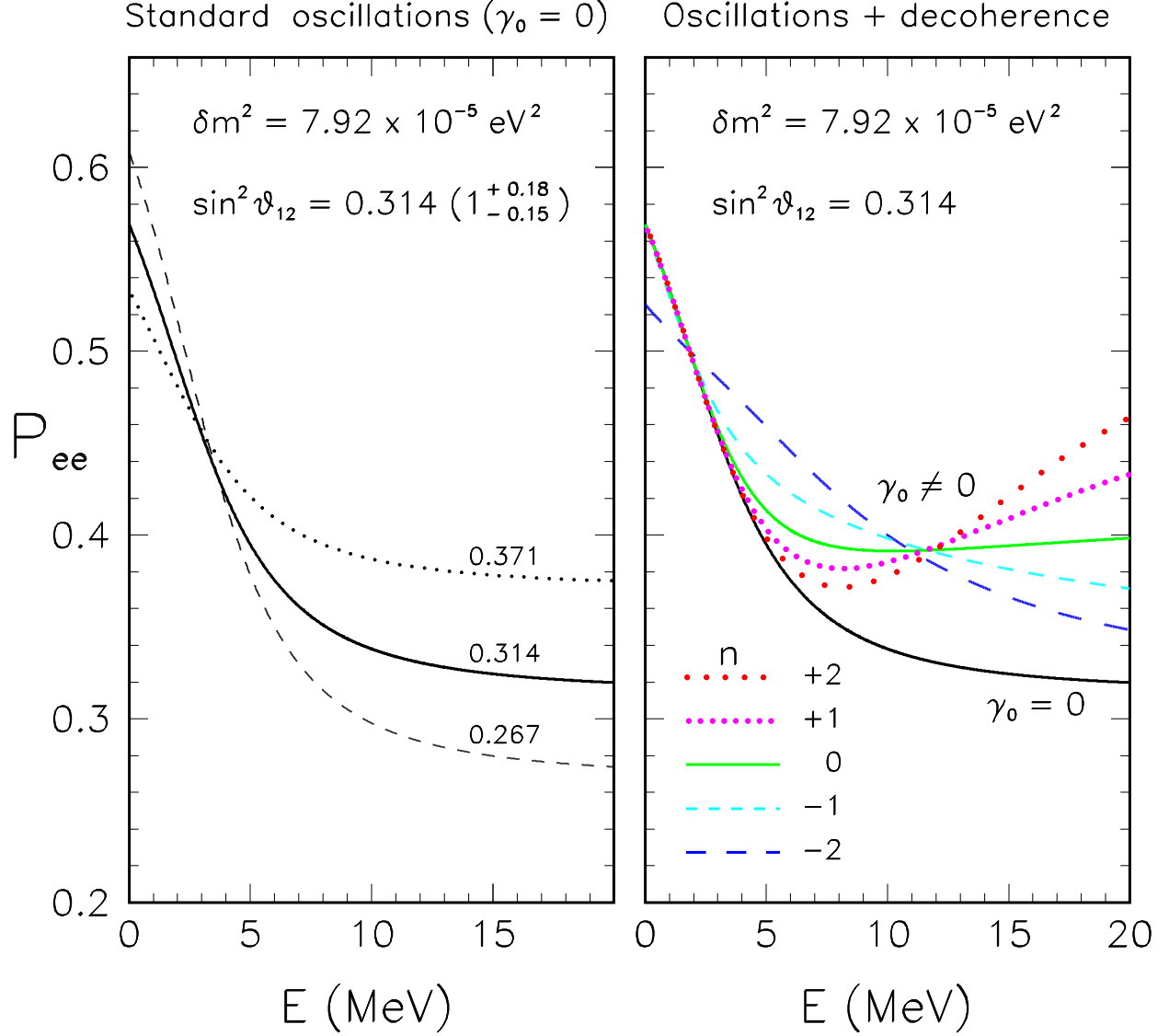


FIG. 2: Energy profile of the (daytime) survival probability of ^8B neutrinos, averaged over their production region in the sun: Comparison of the effects produced by variations of $\sin^2 \theta_{12}$ for $\gamma_0 = 0$ (left panel) and by $\gamma_0 \neq 0$ at fixed $\sin^2 \theta_{12}$ (right panel). In the left panel, $\sin^2 \theta_{12}$ is varied within its $\pm 2\sigma$ limits. In the right panel, for each index $n = [-2, -1, 0, +1, +2]$ the value of γ_0 is taken equal to the corresponding 2σ upper limit (reported in Table I), which in units of 10^{-24} GeV corresponds respectively to: 0.81×10^{-4} ($n = -2$), 0.78×10^{-2} ($n = -1$), 0.67 ($n = 0$), 0.58×10^2 ($n = +1$), 0.47×10^4 ($n = +2$). The curve corresponding to standard oscillations ($\gamma_0 = 0$) is also shown in the right panel as a guide to the eye. In all cases, δm^2 is fixed at its best-fit value.

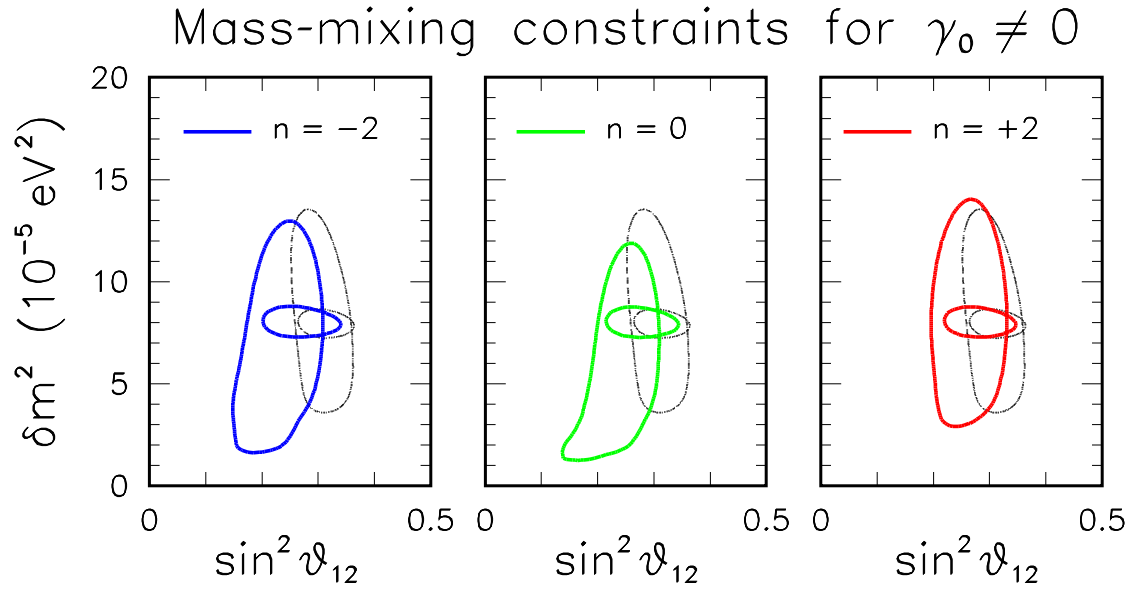


FIG. 3: Constraints on the mass-mixing parameters for $\gamma_0 = 0$ (thin dotted curves) and for γ_0 fixed at its 2σ upper limit in Table I (thick solid curves). The three panels refer, from left to right, to the three cases $n = -2$, 0 , and $+2$. The smaller (larger) allowed regions refer to the solar+KamLAND (solar only) data analysis.

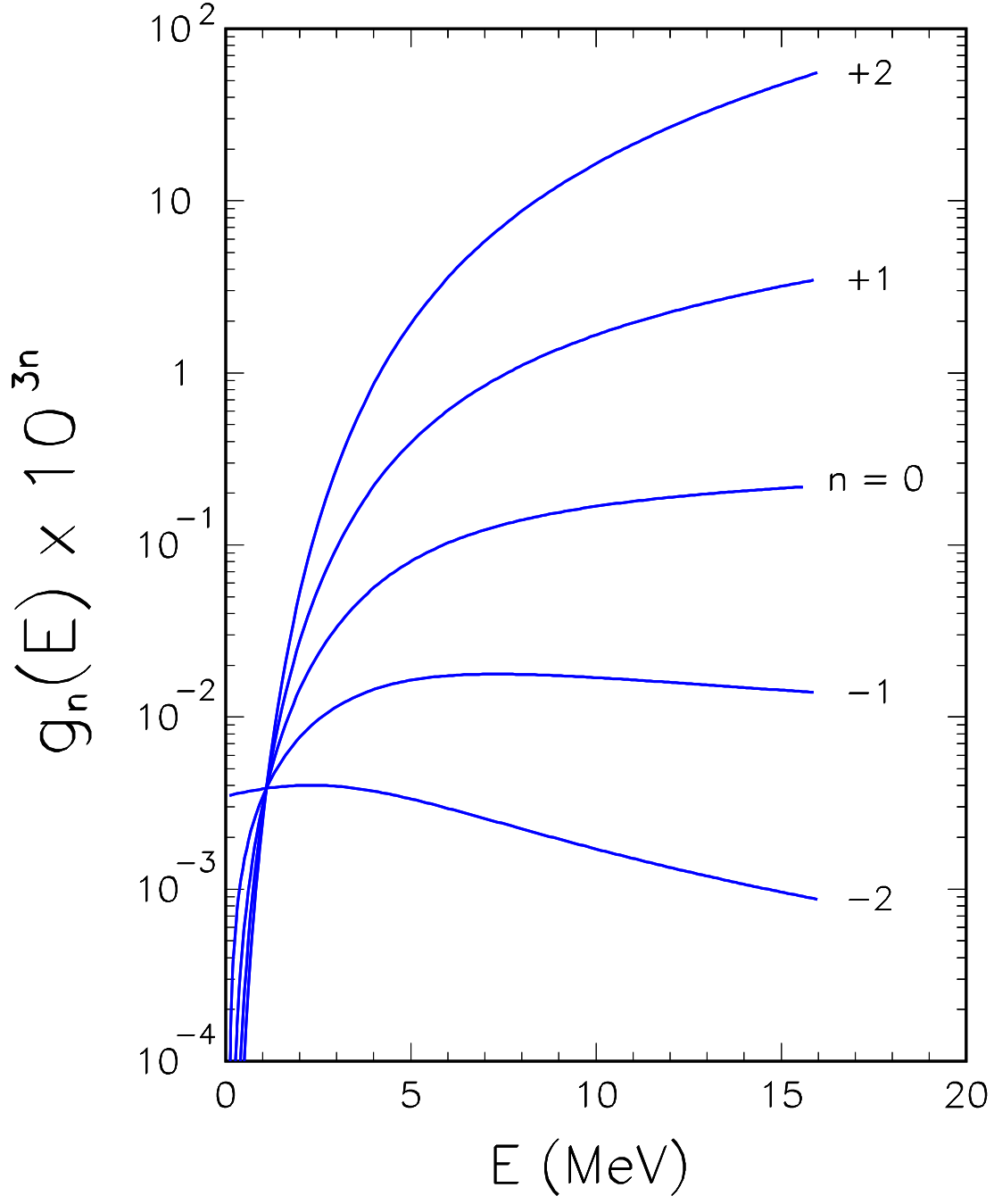


FIG. 4: Energy profile of the auxiliary function $g_n(E)$, which modulates the exponent of the damping factor induced by decoherence in solar neutrino oscillations. The function is multiplied by 10^{3n} for a better graphical view. The shown function refers to a neutrino produced at the Sun center and to best-fit oscillation parameters; altering this choice would induce minor variations. See the text for details.